Available online at www.sciencedirect.com
SCIENCE DIRECT®
Advances in Space Research 37 (2006) 1629–1634
ADVANCES IN SPACE RESEARCH (a COSPAR publication)
www.elsevier.com/locate/asr

Simulation of the role of solar and orbital forcing on climate

Ulrich Cubasch [a,*], Eduardo Zorita [b], Frank Kaspar [c], Jesus F. Gonzalez-Rouco [d], Hans von Storch [b], Kerstin Prömmel [b]

[a] Institut für Meteorologie, Freie Universität Berlin, Carl-Heinrich-Becker-Weg 6-10, 12165 Berlin, Germany
[b] GKSS Research Centre, 21502 Geesthacht, Germany
[c] Max-Planck-Institut für Meteorologie, Model and Data Group, Bundesstr. 53, 20146 Hamburg, Germany
[d] Departmento de Astrofisica y Fisica de la Atmosfera, Universidad Complutense de Madrid, 28040 Madrid, Spain

Received 1 November 2004; received in revised form 27 April 2005; accepted 29 April 2005

Abstract

The climate system is excited by changes in the solar forcing caused by two effects: (a) by variations of the solar radiation caused by dynamical processes within the Sun, and (b) by changes in the orbital parameters of the Earth around the Sun.

Numerical simulations with a three-dimensional coupled ocean–atmosphere climate model have been performed to investigate the sensitivity of the climate system to both kinds of changes in the forcing.

The climate system responds to the (relatively) short term variations of the solar output variations with changes in the surface temperature of up to 2 K, but without any noticeable long lasting effect. The response to the changes in the orbital parameters is more dramatic: dependent if the orbital parameters correspond to the Eemian (a warm phase at around 125 kyr BP) or the one at 115 kyr BP (the onset of the last ice age), the simulation produces a warm state or the initiation of a cold climate. For the Eemian, the simulated climate agrees with the temperature distribution derived from pollen data. For the glacial inception, the model gradually builds up a large snow cover in the northern part of North America.

Keywords: Solar variability; Orbital parameters; Coupled climate models; Climate simulation; Eemian

1. The climate system

The climate system consists of the subsystems atmosphere, oceans (hydrosphere), the ice and snow cover (cryosphere), vegetation (biosphere), the land surfaces (pedosphere) as well as the lithosphere.

The different climate sub-systems fluctuate at different time-scales. These different time-scales determine the time-dependent behaviour and represent therefore the dynamics of the climate system. Fluctuations in the climate system component atmosphere, commonly called "weather", vary at timescales from hours to days, deep sea currents and ice shields vary in time scales from centuries to millennia. As these climate components are interacting with each other, the variability of one sub-system influences the variability of the other sub-systems. In extreme cases, it is therefore possible that a small disturbance is amplified by non-linear processes and has large impacts.

The climate system is driven by external forcings. Here the prime forcing is the solar radiation, but also volcanism counts as external forcing for the climate scientists, as the aerosols emitted by the volcanoes modulate the incoming solar radiation. Mankind influences the climate system via the emission of greenhouse gases, pollutants and land usage.

The solar forcing is only to a first approximation constant. Changes of the orbit of the Earth around the Sun

* Corresponding author. Tel.: +49 30 838 71217; fax: +49 30 838 71160.
E-mail address: cubasch@zedat.fu-berlin.de (U. Cubasch).

0273-1177/$30 © 2005 COSPAR. Published by Elsevier Ltd. All rights reserved.
doi:10.1016/j.asr.2005.04.076

and variations in the solar radiative output represent a time dependent forcing.

In this paper, the response of the climate system (a) to the temporal variability of the solar radiation, anthropogenic emission of greenhouse gases and volcanism, and (b) to varying orbital parameters is studied using a fully coupled ocean atmosphere model. This model is described in Section 2, the experimental conditions are discussed in Section 3. The model results are shown in Section 4, which is followed by a summary (Section 5).

2. The model

The climate model consists of the atmospheric model ECHAM4 (Roeckner et al., 1992) with a horizontal resolution of $3.75° \times 3.75°$ and 19 vertical levels, 5 of them located in the stratosphere, coupled to the ocean model HOPE-G with a horizontal resolution of approx. $2.8° \times 2.8°$ with equator refinement and 20 vertical levels. The ocean and atmosphere models are coupled through flux adjustment to avoid climate drift in long climate simulations. This coupled model has been developed at the Max-Planck-Institute of Meteorology (Legutke and Voss, 1999) and it has been used in many studies of climate variability and climate change (von Storch et al., 2004) as well as paleo climate simulations (Felis et al., 2004; Lorenz and Lohmann, 2004).

3. The experiments

To assess the effect or varying solar radiation on the climate, the model was driven by estimations of variations of the solar constant for the last 1000 years, volcanic activity and concentrations of greenhouse gases (derived from air bubbles trapped in polar ice cores (Etheridge et al., 1996; Blunier et al., 1995)). Annual values of net radiative forcing due to solar variability and volcanic activity were estimated by Crowley (2000) from concentrations of ^{10}Be (a cosmogenic isotope), from historical observations of Sun spots and acidity measurements in ice cores. In the last two centuries the solar component is very close to the Lean data (Lean et al., 1995). Changes in tropospheric sulphate aerosols and ozone concentrations have not been included.

To investigate the effect of the orbital parameters, two simulations using the orbital parameters at 125,000 yr before present (BP) and 115,000 yr BP (see Table 1), which represent different phases of the Eemian interglacial (which was the last interglacial before the present one), have been run.

Compared to the conditions before industrialization (i.e., the time before mankind has begun to influence climate on a large scale) at 125,000 yr BP the combined effect of greater obliquity and eccentricity, together with the fact that perihelion occurred in northern hemisphere summer caused an stronger seasonal cycle of insolation. At 115,000 yr BP the length of perihelion was almost opposite, resulting in a weaker seasonal cycle. Therefore, the selected dates represent phases with approx. maximum and minimum summer insolation on the northern hemisphere. In contrast to the experiments described above, we did not perform transient simulations with variable forcings but so called equilibrium experiments with a constant orbital configuration. The greenhouse gas concentrations (CO_2, CH_4, N_2O) have been adapted to values obtained from Vostok ice cores (Petit et al., 1999; Sowers, 2001). An equilibrium simulation with pre-industrial conditions has been used for comparison, because greenhouse gas concentrations are very similar to the values of the Eemian simulations and therefore the simulated changes can be attributed to orbitally-induced insolation change. All parameters are shown in Table 1.

Table 1
Orbital parameters and greenhouse gas concentrations of the equilibrium simulations

	125 kyr BP	115 kyr BP	Pre-indust
Eccentricity	0.0400	0.0414	0.0167
Obliquity	23.79	22.41	23.44
Precession	127.3	290.9	282.7
CO_2 conc.	270 ppm	265 ppm	280 ppm
CH_4 conc.	630 ppb	520 ppb	700 ppb
N_2O conc.	260 ppb	270 ppb	265 ppb

Orbital parameters are calculated following Berger (1978). Greenhouse gas concentrations are based on Vostok ice cores (CO_2 and CH_4: Petit et al. (1999); N_2O: Sowers (2001)).

4. Results

4.1. The effect of solar variability

The external climate forcing and the simulated global annual near-surface air temperature (SAT), is represented in Fig. 1. The model simulates a temperature maximum around 1100 AD, the Medieval Warm Period (MWP) (Jones et al., 2001), with temperatures very similar to the ones simulated for the present period. The existence of the MWP has been recently a matter of considerable debate, since proxy data have not yielded a consistent picture of its existence (Bradley et al., 2001; Broecker, 2001). In this simulation, the MWP was a global phenomenon, probably caused by the maximum in solar activity in the 12th century. From 1300 AD global temperatures decrease and the simulation enters the so called Little Ice Ice (LIA) lasting until about 1850 AD (Jones et al., 2001). Temperatures in the LIA were about 1 K colder than today's values, the cooling peaking in the Late Maunder Minimum (Eady, 1976) (around

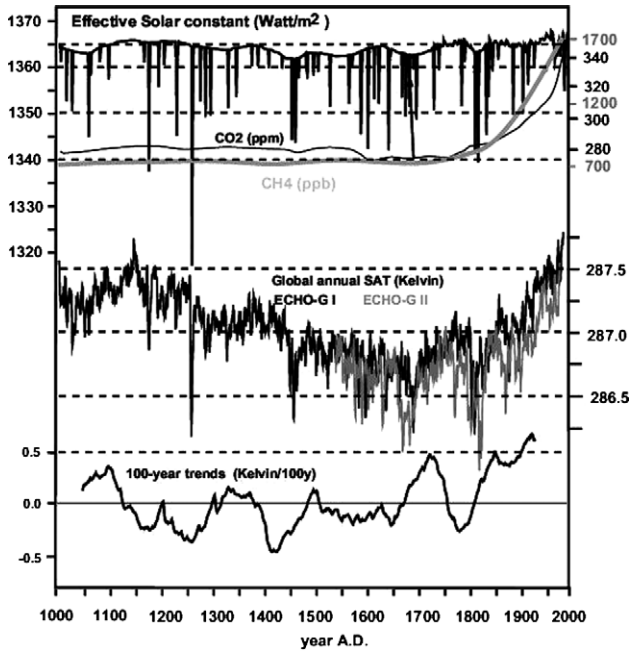

Fig. 1. External forcing effective solar constant and greenhouse gas concentration used to drive the climate model ECHO-G; the simulated global annual surface air temperature (SAT) for two ECHO-G simulations and the running 100-year SAT trends for the 1000-year simulation. The spikes in the effective solar constant represent the effect of volcanic aerosols on the radiative forcing. In 1258–1259 AD, an eruption of unknown location, recorded in the acidity measurements of ice cores, causes a temperature drop of about 1 K.

1700 AD) and the Dalton Minimum (Jones et al., 2001) (around 1820 AD), when simulated temperatures are about 0.25 K colder than the LIA mean. The cooling is a global phenomenon with a regional maxima around a latitude belt of 60°N over land areas (Zorita et al., 2004). Subsequently, global temperatures start increasing almost continuously into the 20th century until the end of the simulation. The simulated secular warming trend in the 20th century is approached, but not surpassed, by warming trends around 1100 AD and in the 18th century. A shorter simulation of the last 500 years with a slightly different model version yields similar results.

The simulated temperature evolution has similar phases of the minima and maxima as the empirical reconstruction by Mann et al. (1999), but with a larger amplitude (up to factor 5), particularly for the LIA and the Dalton Minimum. Other empirical reconstructions based on different proxy data have obtained different amplitudes in variability, depending on the sensitivity of the proxies used (Zorita et al., 2004). For example, the multi-proxy approach of Mann et al. (1999) represents a reconstruction of the annual Northern Hemisphere (NH) temperature, whereas the reconstruction by Esper et al. (2002), based on extratropical dendrochronological data, is more strongly biased towards the NH extratropical summer temperatures. Results by Moberg et al. (2005), in which he used a blend of lake and ocean sediments with tree ring data to estimate the temperature of the last 2000 years show a larger amplitude than the Mann et al. (1999) reconstruction and are closer to the modelled results. This indicates that the issue of the amplitude of surface temperature reconstructions has not yet been settled.

The ECHO-G simulations show a good agreement with a similar simulation of the last 500 hundred years, independently performed at the Hadley Center for Climate Research (Widmann and Tett, 2004).

4.2. Results of the simulation for 125,000 yr BP

At 65°N, the insolation at mid-month June was 11.7% higher than today (531 W/m^2 instead of 475 W/m^2). The insolation of mid-month December was 1.88 W/m^2 compared 3.02 W/m^2 today. A simulation of 2000 years was performed with the modified insolation pattern as constant forcing. After approx. 1000 years the simulation becomes quasi-stationary with respect to ocean-circulation and sea-ice extend. The enhancement of the seasonal cycle in insolation is clearly visible in simulated northern hemispheric temperatures (Fig. 2). Fig. 3 shows the simulated summer temperature as difference to the pre-industrial conditions. The summer near-surface temperature is higher for almost the entire northern hemisphere, in particular over the continents where it is 2 K warmer than during pre-industrial conditions.

A belt with cooler temperatures at around 20°N emerges over Africa and India, which is caused by significantly higher cloud coverage in the summer months. The difference in the percentage of cloud coverage is approx. +10% over Africa at around 20°N and approx.

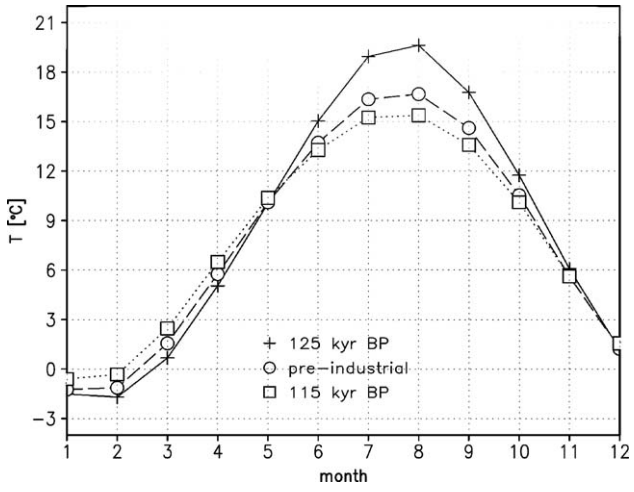

Fig. 2. The annual cycle of temperature in the Northern Hemisphere (20–75°N) for the 125 kyr BP, the 115 kyr BP and the pre-industrial simulation (50 year intervals starting 1200 years after the start of the simulation).

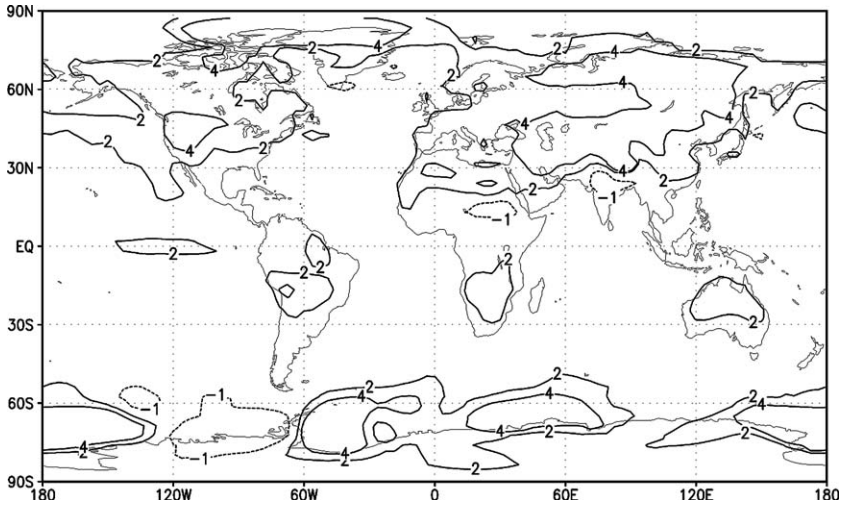

Fig. 3. Mean simulated difference (Eemian at 125 kyr BP minus pre-industrial) of the near-surface temperature in northern summer (JJA).

+25% in the region from the Arabian peninsula to India at around 25°N. In these regions, significantly enhanced westerly winds cause an increase in transport of oceanic moisture into the continents. An increase in summer precipitation of around 2 mm/day is simulated in these regions. These results are consistent with the study of Rohling et al. (2002), who found a northward shift of the Innertropical Convergence Zone during the Eemian summer based on the interpretation of proxy data. Similar results have been obtained in the model experiments by Montoya et al. (2000).

The winter temperatures are lower over the continents with the exception of the area between Eastern Europe and Siberia, where higher temperatures prevail. The general pattern of simulated summer and winter temperatures are in agreement with published datasets of pollen-based reconstructions of European temperatures (Kühl, 2003; Kaspar et al., in press) in displaying higher temperatures than today over most parts of Europe in summer. They show a similar east–west-gradient in winter temperature changes with increasing anomalies towards north-eastern Europe. These higher winter temperatures are in contrast to the reduced winter insolation, but are consistently visible in the reconstructions and simulations. In the simulation two reasons for this pattern can be identified: The sea-ice in the Arctic sea is significantly reduced in both summer and winter. Stronger westerly winds occur over the Atlantic at 60°N which lead to additional advection of oceanic heat into the European continent. As the greenhouse gas concentrations in the simulations are only slightly different, it can be concluded that orbitally induced changes in insolation are sufficient to induce the reconstructed patterns. However, the reconstructed anomalies refer to observed modern climatic conditions where greenhouse gases were already increased. When the Eemian simulation is compared to periods within the 20th century of a transient simulation with the same model, similar patterns are obtained, but they become less distinct for the late decades, because they are blurred by the greenhouse gas effect. The simulated European winter warming was also found in the modelling experiments performed by Felis et al. (2004), who used the same model but with an accelerated transient insolation forcing and calculated the anomalies to a simulation of modern climate.

4.3. Results of the simulation for 115,000 yr BP

At 115,000 yr BP the insolation of mid-month June at 65°N was 7.6% lower (439 W/m^2) than today. At mid-month December it was 6.82 W/m^2, therefore the seasonality of insolation was less strong than today. Again, a consistent reaction of the temperature is apparent, with the strongest differences on the continents. In this simulation, the global annual mean near surface air-temperature cools by 0.08 K/century over the whole simulated interval of 2300 years. It is connected with a continuous increase in northern hemisphere sea ice volume and an expansion of the permanently snow-covered areas over North America (Fig. 4). The northern hemisphere summer sea ice volume is increasing from 28,000 km^3 at the beginning of the simulation to 49,000 km^3 after 2300 simulated years. Due to the reduced insolation an increased meridional temperature gradient occurs. At the end of the simulation the temperature difference between the high and the low latitudes is 47.5 K compared to 42.5 K in the Eemian simulation.

On a global average, the stronger meridional temperature gradient leads to an increased meridional transport of moisture on the northern hemisphere as suggested by Kukla et al. (2002). A comparison of the simulations (125 kyr, 115 kyr, pre-industrial) shows that at 115,000 yr BP a significantly stronger poleward transport of moisture is simulated, in particular over the

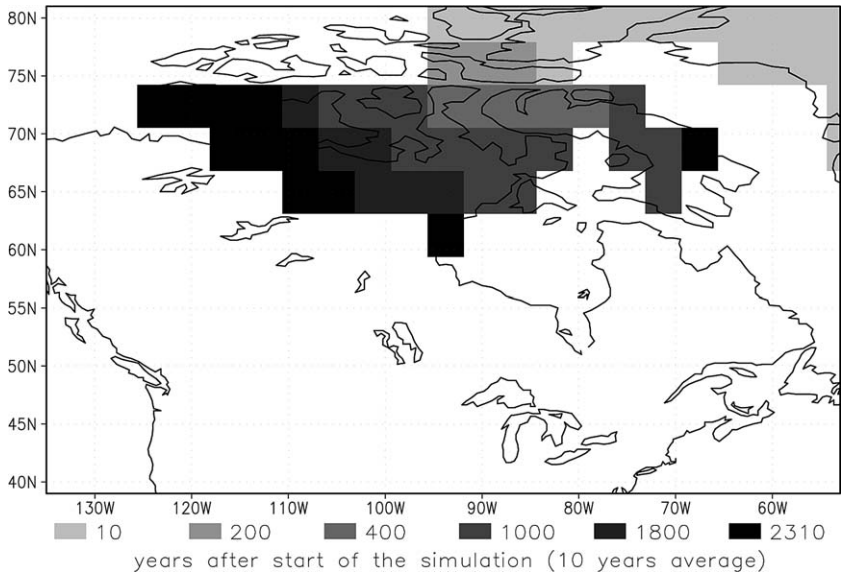

Fig. 4. Expansion of permanently snow-covered areas over North America in the 115 kyr BP simulation. On marked areas snow coverage occurs in all months of the year. The size of the grid boxes corresponds to the spatial resolution of the atmosphere model (~3.75°).

Pacific and Atlantic for the summer months. The decreased summer temperatures combined with the increased moisture availability leads to an increase in snowfall during the summer months and therefore supports the expansion of the snow-covered areas. During the simulated interval a perennial snow coverage occurs on the North American continent only. The accumulation of snow on these areas is a pre-requisite for the build-up of an ice sheet and it indicates that the orbitally induced changes in insolation are sufficient to trigger initial processes of a glaciation. However, since the climate model used does not include an inland ice model, this build-up cannot explicitly be calculated.

5. Summary

The changes in the solar forcing have a noticeable effect on the climate. The solar variability induces climate changes in the order of 1–2 K, thus supporting the findings of Cubasch et al. (1997) and Stott et al. (2000). As these changes in the forcing are comparatively short lived (decades), the climate recovers once the forcing returns to "normal" conditions.

In the case of the forcing by orbital parameters, the climate is substantially altered, since the forcing acts on longer timescales. A "warm" orbital constellation corresponding to the one of the Eemian (125 kyr BP) induces a warmer than present-day climate, while a "cool" orbit corresponding to the conditions of 115 kyr BP forces the climate system toward a significantly colder phase.

For both types of experiments, a number of questions remain:

Why is the amplitude in the case of the model simulation for the last 1000 years for the longer periods substantially larger than what has been derived from the proxy-data reconstructions? Here, the mechanism described by von Storch et al. (2004) might play an important role, i.e., that a reconstruction of the climate by applying regression methods on proxy data underestimates the climate variability. On the other hand, the solar forcing might have been overestimated (Foukal et al., 2004). There are also indications that the snow-vegetation feedback, which could not be simulated due to the lack of a sophisticated vegetation model, would improve the realism of the climate simulation (Claussen et al., 2003).

For the orbital forcing experiments some differences arise between the pollen data reconstructions and the model results, particularly for the precipitation field. The models have problems to simulate precipitation accurately (IPCC, 2001). On the other hand, the reconstruction of the global climate based on local pollen data has a number of deficiencies (Bradley, 1999). Furthermore, in both cases we compare model data, which are representing scales of larger than 500 km with locally derived data (von Storch et al., 1993).

With increasing computing resources, it will in the foreseeable future be possible to simulate either with increased horizontal resolution more regional details, or with the same resolution longer intervals, for example the whole Holocene or the transitions between warm and cold stadials. This leads to a re-assessment and homogenization of the proxy data since the models perform a check on the physical consistency of the data. Accurate information about the solar variability will improve this process.

Acknowledgements

The authors thank S. Legutke and U. Schlese for providing the model and their support in running the simulations. The use of Crowley's, Jones et al. data and data from the NCEP is greatly acknowledged. This work was performed in the frame of the German programme DEKLIM, project REN2000-0786CLI from the Spanish CICYT and the EU project SOAP.

References

Berger, A.L. Long-term variations of daily insolation and Quaternary climate changes. J. Atmos. Sci. 35, 2362–2367, 1978.

Blunier, T., Chappellaz, J.A., Schwander, J., Stauffer, B., Raynaud, D. Variations in atmospheric methane concentration during the Holocene epoch. Nature 374, 46–49, 1995.

Bradley, R.S.. Paleoclimatology. Academic Press, San Diego, USA, 1999, p. 613.

Bradley, S., Briffa, R.K., Crowley, T.J., Hughes, M.K., Jones, P.D., Mann, M.E. The scope of Medieval warming. Science 292, 2011–2012, 2001.

Broecker, W.S. Was the Medieval warm period global?. Science 291, 1497–1499, 2001.

Claussen, M., Brovkin, V., Ganopolski, A., Kubatzki, C., Petoukhov, V. Climate change in Northern Africa: the past is not the future. Climatic Change 57, 99–118, 2003.

Crowley, T.J. Causes of climate change over the past 1000 years. Science 289, 270–277, 2000.

Cubasch, U., Hegerl, G.C., Voss, R., Waszkewitz, J., Crowley, T.C. Simulation with an O-AGCM of the influence of variations of the solar constant on the global climate. Clim. Dyn. 13, 757–767, 1997.

Eady, J.A. The Maunder minimum. Science 192, 1189–1202, 1976.

Etheridge, D., Steele, L.P., Langenfelds, R.L., Francey, R.J., Barnola, J.M., Morgan, V.I. Natural and anthropogenic changes in atmospheric CO_2 over the last 1000 years from air in Antarctic ice and firn. J. Geophys. Res. 101, 4115–4128, 1996.

Esper, J., Cook, E.R., Schweingruber, F.H. Low-frequency signals in long tree-ring chronologies for reconstructing past temperature variability. Science 295, 2250–2253, 2002.

Felis, T., Lohmann, G., Kuhnert, H., Lorenz, S.J., Scholz, D., Pätzold, J., Al-Rousan, S.A., Al-Moghrabi, S.M. Increased seasonality in Middle East temperatures during the last interglacial period. Nature 429, 164–168, 2004.

Foukal, P., North, G., Wigley, T. A stellar view on solar variations and climate. Science 306, 68–69, 2004.

IPCC. in: Houghton, J.T. et al. (Eds.), Climate Change 2001: The Scientific Basis. Cambridge University Press, Cambridge, 2001.

Jones, P.D., Osborn, T.J., Briffa, K.R. The evolution of climate over the last millennium. Science 292, 662–667, 2001.

Kaspar, F., Kühl, N., Cubasch, U., Litt, T. A model-data-comparison of European temperatures in the Eemian interglacial. Geophysical Res. Lett., in press.

Kühl, N. Die Bestimmung botanisch-klimatologischer Transferfunktionen und die Rekonstruktion des bodennahen Klimazustandes in Europa während der Eem-Warmzeit. Dissertationes Botanicae 375. Cramer, Berlin Stuttgart, 2003.

Kukla, G.J., Bender, M.L., de Beaulieu, J.L., Bond, G., Broecker, W.S., Cleveringa, P., Gavin, J.E., Herbert, T.D., Imbrie, J., Jouzel, J., Keigwin, L.D., Knudsen, K.L., McManus, J.F., Merkt, J., Muhs, D.R., Müller, H., Poore, R.Z., Porter, S.C., Seret, G., Shackleton, N.J., Turner, C., Tzedakis, P.C., Winograd, I.J. Last interglacial climates. Quatern. Res. 58, 2–13, 2002.

Lean, J., Beer, J., Bradley, R. Reconstructions of solar irradiance since 1610 - implications for climate change. Geophys. Res. Lett. 22, 3195–3198, 1995.

Legutke, S., Voss, R. The Hamburg Atmosphere-Ocean Coupled Circulation Model ECHO-G. Technical Report 18, DKRZ, Hamburg, Germany, 1999. (Available at: http://www.dkrz.de/forschung/reports.html).

Lorenz, S.J., Lohmann, G. Acceleration technique for Milankovitch type forcing in a coupled atmosphere–ocean circulation model: method and application for the Holocene. Climate Dyn. 23, 727–743, 2004.

Mann, M.E., Bradley, R.S., Hughes, M.K. Northern hemisphere temperatures during the past millennium: inferences, uncertainties, and limitations. Geophys. Res. Lett. 26, 759–762, 1999.

Moberg, A., Sonechkin, D.M., Holmgren, K., Datsenko, N.M., Karlèn, W. Highly variable Northern Hemisphere temperatures reconstructed from low- and high-resolution proxy data. Nature 433, 613–617, 2005.

Montoya, M., von Storch, H., Crowley, T.J. Climate simulation for 125 kyr BP with a coupled ocean–atmosphere general circulation model. J. Climate 13, 1057–1071, 2000.

Petit, J.R., Jouzel, J., Raynaud, D., Barkov, N.I., Barnola, J.M., Basile, I., Bender, M., Chappellaz, J., Davis, J., Delaygue, G., Delmotte, M., Kotlyakov, V.M., Legrand, M., Lipenkov, V.M., Lorius, C., Pépin, L., Ritz, C., Saltzman, E., Stievenard, M. Climate and atmospheric history of the past 420,000 years from the Vostok ice core – Antarctica. Nature 399, 429–436, 1999.

Roeckner, E., Arpe, K., Bengtsson, L., Brinkop, S., Dümenil, L., Esch, M., Kirk, E., Lunkeit, F., Ponater, M., Rockel, B., Sausen, R., Schlese, U., Schubert, S., Windelband, M. Simulation of the present-day climate with the ECHAM model: Impact of model physics and resolution. Report No. 93, Max-Planck-Institute for Meteorology, Hamburg, Germany, 1992.

Rohling, E.J., Cane, T.R., Cooke, S., Sprovieri, M., Bouloubassi, I., Emeis, K.C., Schiebel, R., Kroon, D., Jorissen, F.J., Lorre, A., Kemp, A.E.S. African monsoon variability during the previous interglacial maximum. Earth Planet Sci. Lett. 202, 61–75, 2002.

von Storch, H., Zorita, E., Cubasch, U. Downscaling of global climate change estimates to regional scales: an application to Iberian rainfall in wintertime. J. Climate 6, 1161–1171, 1993.

von Storch, H., Zorita, E., Jones, J., Dimitriev, Y., Gonzalez-Rouco, F., Tett, S. Reconstructing past climate from noisy data. Science 306, 679, 2004.

Sowers, T. N_2O record spanning the penultimate deglaciation from the Vostok ice core. JGR Atmos. 106 (D23), 31903–31914, 2001.

Stott, P.A., Tett, S.F.B., Jones, G.S., Allen, M.R., Mitchell, J.F.B., Jenkins, G.J. External control of 20th century temperature variations by natural and anthropogenic forcings. Science 15, 2133–2137, 2000.

Widmann, M., Tett, S.F.B. Simulating the climate of the last millennium. IGBP Newslett. 56, 10–13, 2004.

Zorita, E., von Storch, H., Gonzalez-Rouco, F., et al. Climate evolution in the last five centuries simulated by an atmosphere–ocean model: global temperatures, the North Atlantic Oscillation and the Late Maunder Minimum. Meteor. Z. 13, 271–289, 2004.